Am J Transl Res 2018;10(12):4030-4041
www.ajtr.org /ISSN:1943-8141/AJTR0076902

*Original Article*

# Improved biphasic calcium phosphate combined with periodontal ligament stem cells may serve as a promising method for periodontal regeneration

Han Shi, Wenyi Zong, Xiaoyu Xu, Jingqian Chen

*Department of Orthodontics, School & Hospital of Stomatology, Tongji University, Shanghai Engineering Research Center of Tooth Restoration and Regeneration, Shanghai 200072, China*

Received March 28, 2018; Accepted November 9, 2018; Epub December 15, 2018; Published December 30, 2018

**Abstract:** The study aimed to investigate if a construct of porous improved biphasic calcium phosphate (BCP) combined with osteogenically induced periodontal ligament stem cells (PDLSCs) could repair periodontal defect. Human PDLSCs were cultured, identified, and osteogenically induced, and then seeded on the improved BCP, assessed by scanning electron microscopy and MTT method. Afterwards, PDLSC-seeded scaffolds were used in six Beagle dogs' alveolar bone dehiscence model, and new bone formation was assessed by three-dimensional micro-computed tomographic imaging, fluorescence, and light microscopy at 4$^{th}$, 8$^{th}$ and 12$^{th}$ week postoperatively. Results showed that PDLSCs were positive for STRO-1 and vimention, while negative for cytokeratin. They had the capacity to undergo osteogenic differentiation *in vitro*. When seeded on the improved BCP, PDLSCs exhibited significantly great viability. The use of PDLSC-seeded improved BCP promoted effective periodontal regeneration. In conclusion, this study demonstrates the potential of improved BCP combined with PDLSCs as a promising method for periodontal regeneration.

**Keywords:** Periodontal ligament, stem cells, biphasic calcium phosphate, scaffold materials, tissue engineering

## Introduction

Periodontitis is a common and widespread disease that causes destruction of peridontium including alveolar bone, periodontal ligament, and cementum. Tissue engineering aims to restore the structures of lost periodontium. The principles of tissue engineering for regeneration involve the combination and interaction of three major elements, known as scaffolds, cells, and biochemical factors [1]. It involves the seeding of cells onto a scaffold *in vitro* and then implanted into the body as prosthesis when matured [2]. The natural tissue regeneration processes then take place, blood vessels infiltrate the structure and the scaffold eventually degrades leading to newly formed tissue in place.

A scaffold is used to create the three-dimensional organization needed for appropriate cell interactions and favoring flow of nutrients for cell growth. It should also have osteoconductive properties, supporting cells through a suitable surface chemistry [3, 4]. Biphasic calcium phosphate (BCP) bioceramics, which are made up of hydroxyapatite (HA) and β-tricalcium phosphate (β-TCP) with different proportions, are recommended for use as dental applications due to their excellent bioactivity [5]. Consequently their degradability can be manipulated through phase composition, porosity, proliferation, leading to the formation of more biocompatible, osteoconductive and in some cases, osteoinductive ceramics, which can favor increased bone formation [6-9]. A BCP made of HA and β-TCP at the weight ratio of 40:60 was obtained using a technique integrating the gel casting with polymer sponge methods [10]. Shi et al. [11] named it improved porous BCP ceramic for its more reasonable pore diameter, pore wall thickness and porosity. They proved that the BCP had biocompatibility and was able to act as a stable scaffold to induce periodontal regeneration effectively.

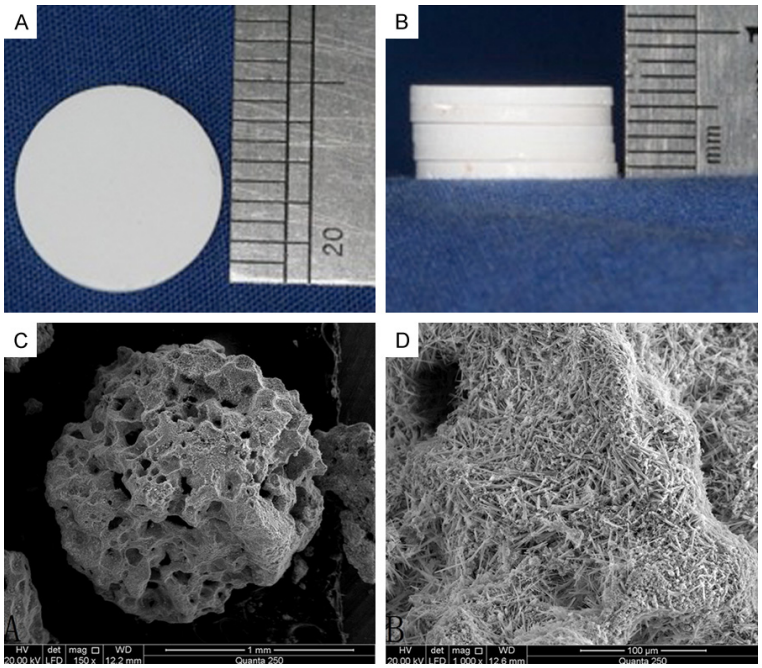


**Figure 1.** The structure of the porous improved biphasic calcium phosphate (A, B: original) at different magnification (C: × 150, D: × 1000).

The other vital factor of tissue regeneration is cells. Byoung-Moo Seo et al. first defined the postnatal PDLSCs as stem cells in 2004. Their findings showed that postnatal PDLSCs were clonogenic, highly proliferative and capable of regenerating cementum/PDL-like tissues [12]. There were further findings indicated that PDL cells possess crucial stem cell properties, such as self-renewal and multi-potency, and express the mesenchymal stem cell markers CD105, CD166, and STRO-1 on their cell surface [13]. Consequently, PDLSCs are deemed as have potential for use in periodontal tissue regeneration. Further study showed periodontal regeneration was significantly observed with both newly formed cementum and well-oriented PDL fibers more in the PDLSC group than in the alveolar periosteum or bone marrow-derived cells groups [14].

In this study, we treated the periodontal defect with the compound of improved BCP and PDLSCs obtained *in vitro* to assess its efficacy in tissue regeneration.

## Materials and methods

### *Biomaterial preparation*

In this study, the improved porous BCP ceramic was made of hydroxiapatite (HA) and β-tricalcium phosphate (β-TCP) at weight ratio of 40:60, grain size was controlled by changing the time and temperature of BCP precipitation; specifically, the BCP containing solution was stirred at room temperature for 24 h. Each BCP-containing solution was then centrifuged, filtered, dried at 60°C for 8 h, heated in air at 10°C/min from room temperature to a final temperature of 1200°C, and sintered at this temperature for 60 min. Then BCP samples were cut to cube (**Figure 1A** and **1B**).

The improvement of BCP was primarily reflected in its high porosity, and its minimum pore size was almost to a nanometer scale in three-dimensional space. Scanning electron micrographs of the improved BCP reveal that the pore distribution of BCP ceramic was uniform, microporous distributed widely in the wall of macroporous. Macroporous diameter was 300-500 μm or so (original magnification: × 150, **Figure 1C**), minimum microporous size was almost less than 100 nm (original magnification: × 1000, **Figure 1D**). Through micro-computed tomography (μCT 80, Scanco Medical AG, Basserdorf, Swiss) analysis, the improved BCP exhibited a reasonably homogenous structure with the volume porosity of 85%, mean pore diameter of 162 μm (range, 116-515 μm) and pore wall thickness of 66 μm (range, 36-144 μm). All the pores were intercommunicated, its microstructure features thus could fully guarantee the access of nutrients and ideally encourage angiogenesis and neovascularization into the defect region. BCP samples were degreased, ultrasonically cleaned and sterilized in a steam autoclave at 120°C for 30 min according to standard laboratory procedures.

### *Animal preparation*

Six healthy adult male beagle dogs about 2 years old and 16.7±2.1 kg weight were enrolled in this study. They were supplied by the Experimental Animal Centre of Shanghai Jiaotong University (Shanghai, China). The study

protocol was approved by the Animal Ethical Committee for Animal Research of Sichuan University (Shanghai, China). During the experiment, animals had free access to feed and water, and got accustomed with the environment 1 week prior to the operation.

*PDLSCs collection*

The teeth were collected from clinically healthy premolars extracted for orthodontic reasons, and written informed consent was obtained from each participant. The PDL was gently separated from the middle third of the root surface. After separation, PDLSC culture was performed in accordance with the modified tissue culture technique. Briefly, PDL was minced into 1 mm 3 cubes, covered with coverslip, and maintained in Delbecco's modified Eagle medium (DEME; Hyclone, USA) containing 10% fetal bovine serum (FBS; Gibco), 100 U/mL penicillin, and 100 U/mL streptomycin. The resultant cell suspension was then seeded in 25-ml flasks and incubated at 37°C in humidified air with 5% $CO_2$. Confluent cells were trypsinized and serially subcultured. Collect the cells on the third passage ($2 \times 10^7$) in 2 mL of culture medium were incubated with monoclonal mouse anti-human STRO-1 (Abcam, USA) at a dilution of 1:100 (Serotec) for 30 min at 4°C. Unbound antibody was removed by washing twice with PBS and the cells were resuspended in 2 ml of cell culture medium containing anti-human STRO-1 magnetic beads, incubated for 30 min at 4°C. Cells were separated from the beads with magnetic frame, washed by PBS three times, and incubated ($2 \times 10^4$) in primary medium.

*Immunohistochemistry staining*

Cells incubated in 6-well plates ($2 \times 10^5$) were fixed in 4% paraformaldehyde for 10 min. Monoclonal mouse anti-human vimention (Boster, Wuhan), cytokeratin (Boster, Wuhan) and STRO-1 were used. Immunohistochemical staining was carried out using SABC method and a commercially available kit: washed by PBS 5 min, treated with methanol containing 3% hydrogen peroxide for 10 min, washed by PBS again, applied with blocking serum for 10 min, incubated in anti-vimention monoclonal antibody (1:300), anti-cytokeratin monoclonal antibody (1:300), anti-SRTO-1 monoclonal antibody (1:100) overnight at 4°C. Negative control sections were incubated with PBS instead of the primary antibody. After washing in PBS, a biotin-marked secondary antibody was applied for 30 min at 37°C followed by peroxidase-marked streptavidin for an additional 20 min. Washed by PBS for 15 min, colored using DAB color kit. Haematoxylin redyed, dehydrated, been transparent, sealed and observed by Microscope.

*Osteogenic differentiation of PDLSC*

PDLSCs collected were incubated in the osteogenic medium (DEME containing 10% (v/v) FBS, 100 U/mL penicillin, 100 U/mL streptomycin, 10-8 M dexamethasone, 10 m Mb-phosphoglycerol, and 50 mM L-2-ascorbic acid; Sigma). The cells after second passages were used for the animal experiment. ALP staining was tested after 7 days of culture in the osteogenic medium. The cells were fixed for 10 min at 4°C and then incubated with a mixture of naphthol AS-MX phosphate and fast blue BB salt (ALP kit; Hongqiao). The alizarin red staining was performed after 21 days of culture under the osteogenic medium. The cells were fixed with 10% formalin and stained with 40 mM alizarin red solution for 30 min at 37°C. For assessment of quantitative ALP activity, the assay was conducted after 4 and 7 days. Briefly, cells were washed twice with PBS and suspended in lysis buffer with 0.1 mL of 0.2% NP-40, and then were mixed with 0.1 mL of 1 mg/mL p-nitrophenyl phosphate (Sig-ma) in 1 M diethanolamine buffer. After incubation at 37°C for 15 min, the reaction was stopped by the addition of 3 N NaOH. Enzyme activity was quantified by absorbance at 405 nm. Total protein content was determined with the Bradford method by using the Bio-Rad protein assay kit (Bio-Rad), and a series of bovine serum standards. ALP activity was normalized by the Protein content and expressed as Abs/mg-protein.

To detect mineralization, cells on days 14 and 21 were washed five times in PBS and fixed in cold 70% ethanol for 1 h. The cells were washed three times with $dH_2O$ and stained with 40 mM alizarin red solution for 20 min at room temperature, and then the stain was desorbed with 10% cetylpyridinium chloride (Sigma) for 1 h. Finally, the dye was collected and mineralization was quantified by absorbance at 590 nm (Elx800; Bio-Tek) as described in previous study. All experiments were done in triplicate.

*Cell seeding on the improved BCP*

Sterilized particulate improved BCP with macropore diameter of 300-500 μm (State Key Laboratory of Oral Diseases, Sichuan University) was used as scaffold. Cells cultured in osteogenic medium were detached from culture dishes using 0.25% trypsin/ethylenediaminetetraacetic acid, centrifuged, and then resuspended in the medium without FBS at a density of $2 \times 10^7$ cells/mL, and then PDLSCs suspension was dropped onto the BCP by means of the pipetting technique and incubated in the 24-well plate at 37°C for 4 h as previously described. The PDLSCs/BCP constructs were then cultured in the osteogenic medium; cell spreading on the scaffolds was detected under scanning electron microscopy (Quanta 250, FEI, Hong Kong) at 6 h, 12 h, 24 h, 36 h and 48 h after cell seeding. Cell viability was determined using the tetrazolium salt MTT (3-[4,5-dimethylthiazol-2-y1]-2,5-diphenyltetrazolium bromide) assay when PDLSCs were seeded into each scaffold in 24-well plastic culture plates and incubated for 2, 5, and 7 days. Specimens were then gently rinsed with phosphate-buffered solution and transferred into new 24-well culture plates. Next, 100 μL of MTT solution (5 mg/mL) was added into each well and incubated at 37°C for 4 hours. The medium was then removed and 750 μL of dimethylsulfoxide was added. Finally, 150 μL of MTT solution was transferred to a 96-well plate. The absorbance value was measured in a multiwell spectrophotometer at 490 nm.

*Surgical procedure*

Animals were anesthetized by intravenous injection of pentobarbital (pentobarbital, shanghai, China; 30 mg/kg). After shaving and disinfection preparation, 12 dehiscences were to be produced on the buccal aspect of bilateral lower second premolars of the 6 beagle dogs. At first, a full-thickness, mucoperiosteal flap was reflected and elevated to expose the buccal aspect of lower second premolars (P2), and then a rectangular piece of the buccal alveolar bone, 3 mm wide and 5 mm long, and deep enough to expose the root surfaces, was removed with a bone chisel. The dimension of the defect was verified with a periodontal probe. A reference notch was made on the root surface at the bottom of the bone dehiscence. Defects were rinsed thoroughly with sterile saline. After PDLSCs/BCP constructs were immersed into the animal's blood, the left dehiscences were filled with PDLSCs/BCP constructs and covered with Biog-Gide membrane (Geistlich Pharma AG, Swiss), while the contral aterals were treated with OFD as controls. Finally, the flap was repositioned and sutured with Gore-Tex CV-5 suture (W.L. Gore & Associates, Flagstaff, AZ), and periodontal dressing placed to protect the wound and promote tissue healing. Postoperative antibiotic treatment was conducted twice daily for 3 consecutive days with 30,000 IU of penicillin G and 6 mg of gentamycin per kilogram of body weight. Plaque control was maintained throughout the experimental period by topical application of 0.2% solution of chlorhexidine gluconate spray (Hibitane concentrate, Sumitomo, Osaka, Japan) three times a week. The sutures were removed 2 weeks after the operation. At the end of experiment they were sacrificed with an overdose of sodium pentobarbital (pentobarbital, shanghai, China) through the cephalic veins. Three dogs were used at week 4, 8 and 12 respectively. Block sections of the teeth including alveolar bone and soft tissue were removed and fixed for 48 h in 4% paraformaldehyde solution, and then were dehydrated in a graded ethanol series.

*Fluorescence labeling*

The animals received polychrome sequence fluorescence labeling according to the following scheme: Oxytetracy-cline (Sigma-Aldrich, Munich, Germany), 20 mg/kg body weight, intravenous, 3 weeks post-operation; Calcein Green (Sigma-Aldrich, Munich, Germany), 16 mg/kg body weight, intravenous, 6 weeks post-operation; Xylenol Orange (Sigma-Aldrich, Munich, Germany), 34 mg/kg body weight, intravenous, and 9 weeks post-operation.

*Three-dimensional micro-computed tomography (Micro-CT) analysis*

The samples were firstly trimmed to proper size for the analysis chamber of the Micro-CT device (Scanco Medical AG, Swiss), and then were mounted on a turntable that could be shifted automatically in the axial direction. Six hundred projections were taken over 180° or 360° of object rotation. The X-ray shadow projections were digitized as 1024 × 1024 pixels with 4096 brightness gradations (12 bit) for cooled cam-

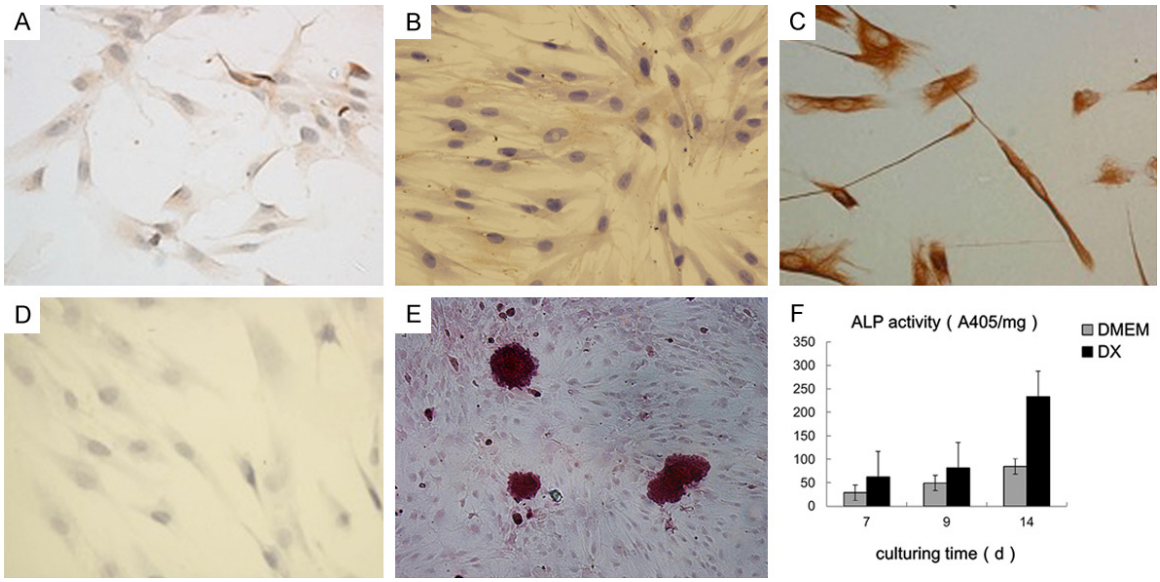


**Figure 2.** The identification of the PDLSCs: the cells formed adherent clonogenic cell clusters of fibroblast-like cells (A), positive for STRO-1 (B) and vimention (C), while negative for cytokeratin (D) Multiple nodules were observed in the osteogenic medium after stained with alizarin red (E). Cells in the osteogenic medium present a greater ALP activity (F).

era or 256 gradations (8 bit). The spatial resolution obtained was 10 um.

*Histological examination*

The samples were firstly trimmed to proper size and fixed in 4% buffered paraformaldehyde (pH 7.4) for 4 days. The central parts of the samples containing the second premolars were dehydrated in ascending concentrations of alcohols from 75% to 100%. Finally, the samples were embedded in polymethylmethacrylate (Sigma) for 14 days before polymerization. The specimens were cut into 500-um-thick sections using diamond-coated internal-hole saw microtome (Leica SP1600), and were subsequently ground and polished to a final thickness of about 40 um for the observation of fluorescent labeling using a confocal laser scanning microscope (Leica TCS Sp2 AOBS) and Van-Geision staining using optical microscope (Olympus BX5, Germany). High resolution, low magnification of 4, and digital fluorescent micrographs were made through transmission light (DAPI-, FITC- and rhodamine-type filter sets for Oxytetracycline, Calcein Green and Xylenol Orange fluorescence, respectively), and then combined with digital image acquisition. The images of the Van-Geision staining sections were captured by a digital camera connected to that light microscope with a magnification of 100.

*Masson staining*

Tissue slices were removed from plastic and put into distilled water. The slices were stained in hematoxylin for 5 to 10 minutes, and then put into hydrochloric acid alcohol for differentiation. Then the slices were washed by running water for blueness and then washed by distilled water. The slices were stained in ponceau acid fuchsin for 5 to 8 minutes. Then the slices were washed by distilled water. The slices were stained in 1% phosphomolybdic acid for 1 to 3 minutes. Then the slices were put into aniline blue for 5 minutes directly without washing. At last, the slices were washed quickly, and then dried at incubator of 60°C. Then, the slices were handled with xylene for transparency and fixed in natural resin.

## Results

*Characteristics of PDLSCs*

To identify the PDLSCs, single-cell colonies were generated from human periodontal ligament-derived cells, which formed adherent clonogenic cell clusters of fibroblast-like cells (**Figure 2A**). These colony-forming cell popula-

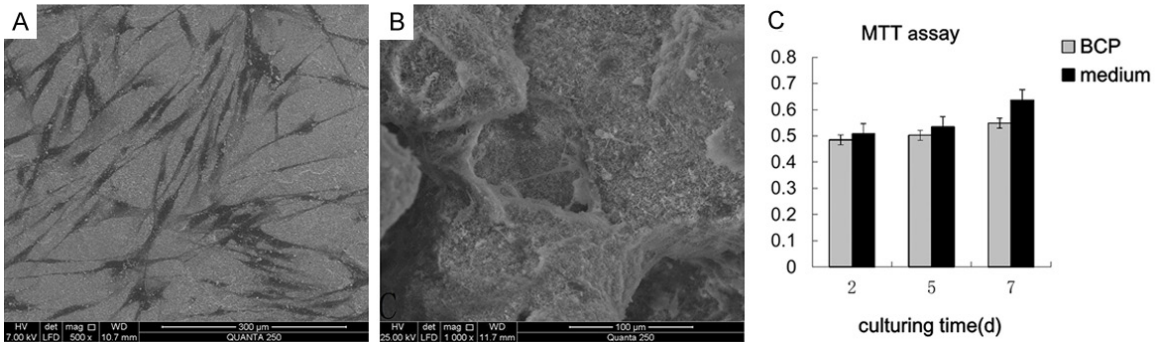


**Figure 3.** 36 h after cell seeding on the surface of the scaffold (A: × 150, B: × 1000); MTT assay showed that there was no significant difference between cells on the BCP and in the medium (C).

tions were termed PDLSCs. The progeny of PDLSCs exhibited typical spindle-shaped fibroblast-like morphology and were positive for STRO-1 and vimention, while negative for cytokeratin (**Figure 2B-D**). Multiple nodules were observed in the osteogenic medium after stained with alizarin red (**Figure 2E**). Cells in the osteogenic medium present a greater ALP activity (**Figure 2F**).

*Cell seeding and activity on the improved BCP*

The PDLSCs were seen spreading well on the surface of the scaffold *in vitro* 36 h after cell seeding (**Figure 3A** and **3B**). MTT assay showed that there was no significant difference between cells on the BCP and in the medium (**Figure 3C**).

*Micro-CT analysis*

*Qualitative analysis*: When the reference notch at the buccal aspect of P2 root surface became invisible in the reconstructed 3D images of the teeth together with its surrounding alveolar bone of PDLSCs/BCP group (**Figure 4A** and **4B**) suggested that the defect region had new bone formation and the notch had been covered by newly formed bone. However, the reconstructed images of OFD controls, regardless of the week 4 or the week 12 group, revealed the reference notch clearly, meaning that no new bone formation had occurred (**Figure 4C** and **4D**). At the week 4 PDLSCs/BCP group, the 3D reconstruction images of BCP groups displayed that the defect region was filled with the mixture of bone matrix and material, which had not fully degraded yet. Its surface was rough and uneven, similar to the scaffold material, but showed significant difference with the neighbor bone tissues (**Figure 4A** and **4B**). At the week 8 PDLSCs/BCP group, the defect region had new visible bone formation, while still had a small amount of scaffold material left (**Figure 4E** and **4F**). At the week 12 PDLSCs/BCP group, the defect region had obvious new bone formation and the bone had regenerated close to its original height (**Figure 4G** and **4H**).

*Quantitative analysis*: The visual assessment on structural images of bone and biomaterial, morphometric parameters were determined from the micro-tomographic data sets using direct 3D morphometry [15, 16]. Through selecting the same volume of host bone and newly formed bone in the experimental groups and calculating with triangulation (TRI) method, the differences between them were found (**Table 1**). With the extension of experimental period, the degree of maturity of new bone was also increased and approximated to host bone all the more.

*Fluorescence microscopy*

Fluorescence labeling was applied to visualize newly formed bone tissues. And sequential fluorochrome labels revealed the dynamics of bone formation. Fluorochrome deposited together with calcium in the bone formation process. Oxytetracycline, Calcein Green and Xylenol Orange were present in the healing bone of the transverse process and marked the areas of bone tissue regeneration in order. At the 12$^{th}$ week of PDLSCs/BCP group, the formation of new bone was apparent, and the labeling area was almost occupied by yellow and light green, while the line of Xylenol Orange displayed red at the outer bone (**Figure 5A**). In OFD group, no bone formation could be seen but a notch on the root surface and migratory epithelium (**Figure 5B**).

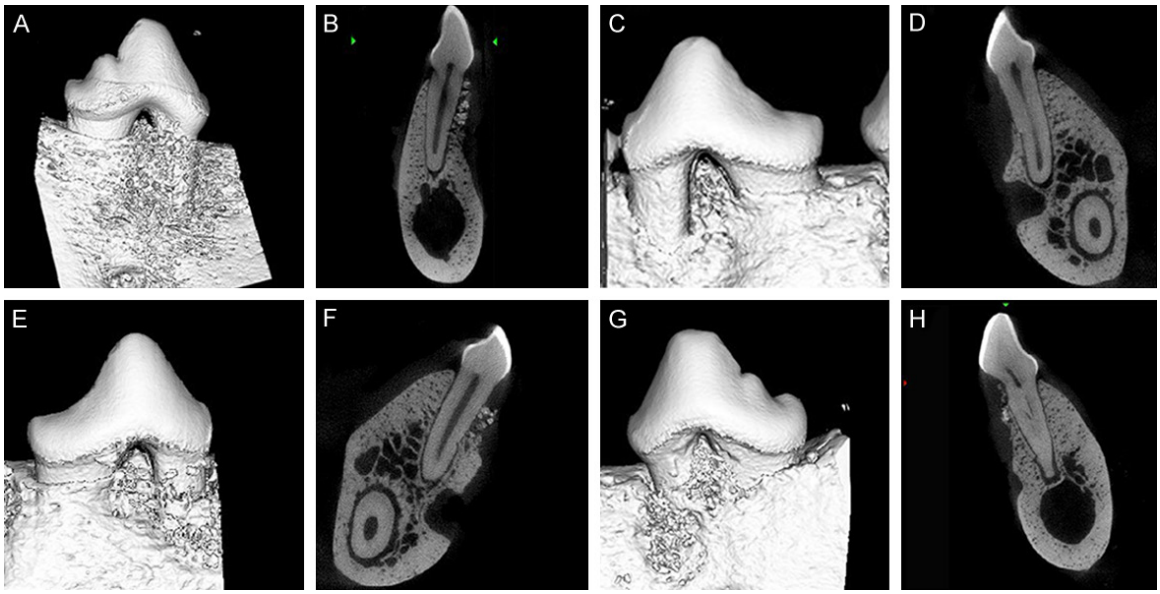


**Figure 4.** The reconstructed 3D images of the teeth together with its surrounding alveolar bone of PDLSCs/BCP group at 4th week (A, B), 8th week (E, F), 12th week (G, H), and that of the OFD group (C, D).

**Table 1.** Quantitative results about newly formed bone of experimental group (TRI)

| | BV ($mm^3$) | TV ($mm^3$) | BV/TV (%) | Tb.N 1/mm | Tb.Th μm | Mean Density (mg HA/ccm) |
|---|---|---|---|---|---|---|
| 4 w | 0.0208 | 0.0861 | 24.09 | 0.3122 | 0.0956 | 459.12±147.47 |
| 8 w | 0.0481 | 0.0866 | 55.54 | 2.4073 | 0.1601 | 847.56±139.23 |
| 12 w | 0.0718 | 0.0891 | 80.21 | 3.2661 | 0.2685 | 795.83±154.59 |
| HB | 0.0798 | 0.0859 | 93.46 | 3.9468 | 0.2793 | 975.88±149.53 |

BV: new bone volume; TV: total volume; BV/TV: relative bone volume; Tb.N: trabecular number; Tb.Th: trabecular thickness; HB: host bone (as control). μCT scanning was progressed at 4, 8 and 12 weeks after implantation.

*Histological analysis*

Based on the light microscopy analysis of specimens stained with Van Gieson's picro fuchsin, the formation of new bone in the PDLSCs/BCP group was apparent. At the 4th week, close observation of bone formation showed osteoid tissues secreted by osteoblast-like cells was growing into the material. The large number of pores, found in the newly formed tissues, was the undegradable BCP. At the 8th week, newly formed bone matrix, osteocytes, and mineralized bone were observed on the host bone bed. New cementum had deposited on the old cementum and root planed dentin. At the 12th week, the alveolar bone in the bone dehiscence was reformed and the PDL were reorganized. Collagen fibers were observed adjacent to the newly formed cementum, and most of them were inserted into cementum and adjacent bone at right angles. In the OFD group, the newly-formed bone near the notch were invisible, with only epithelium and connective tissue covering the notch for periodontal repair instead of regeneration at 12th week after operation (**Figure 6A-H**).

*Masson staining*

Masson staining could reveal maturity of bone and collagen. This study aimed to compare the regeneration of bone and collagen between the 8th and 12th week after operation during periodontal regeneration period, when scaffold materials transformed into new bone. At the 8th week in experimental group, alveolar bone was mainly blue, the fibers were compact which were hard to distinguish directions, and the shape of vessel lumen was irregular (**Figure 7A**). At the 12th week in experimental group, alveolar bone was red and blue, turning into red when compared with the 8th week, and the Havers' system was shown. The fibers were compact and regular. Abundant vessels were shown (**Figure 7B**).

## Discussion

Bone tissue engineering (BTE) was introduced, involving the preoperative seeding of the scaf-

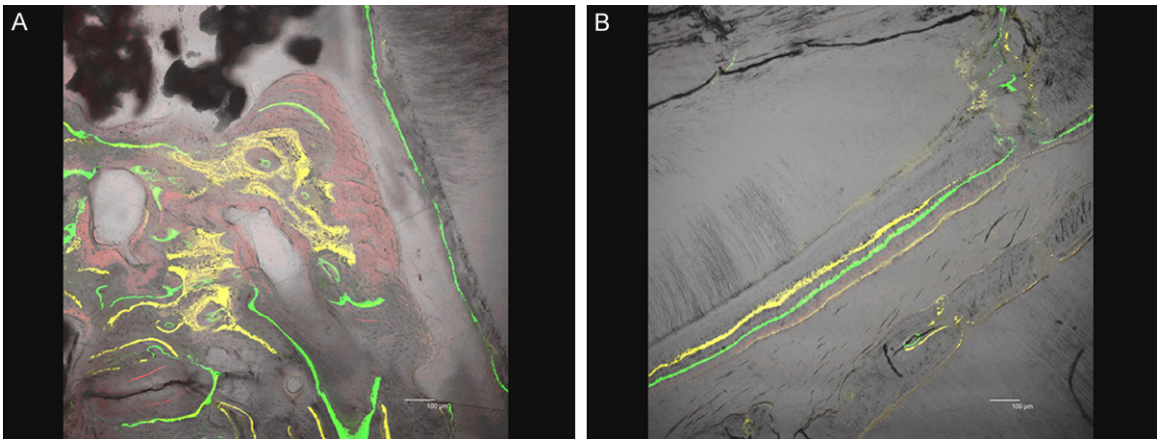


**Figure 5.** Fluorescence labeling to visualize the newly formed bone tissues at the 12th week of PDLSCs/BCP group (A) and the OFD group (B).

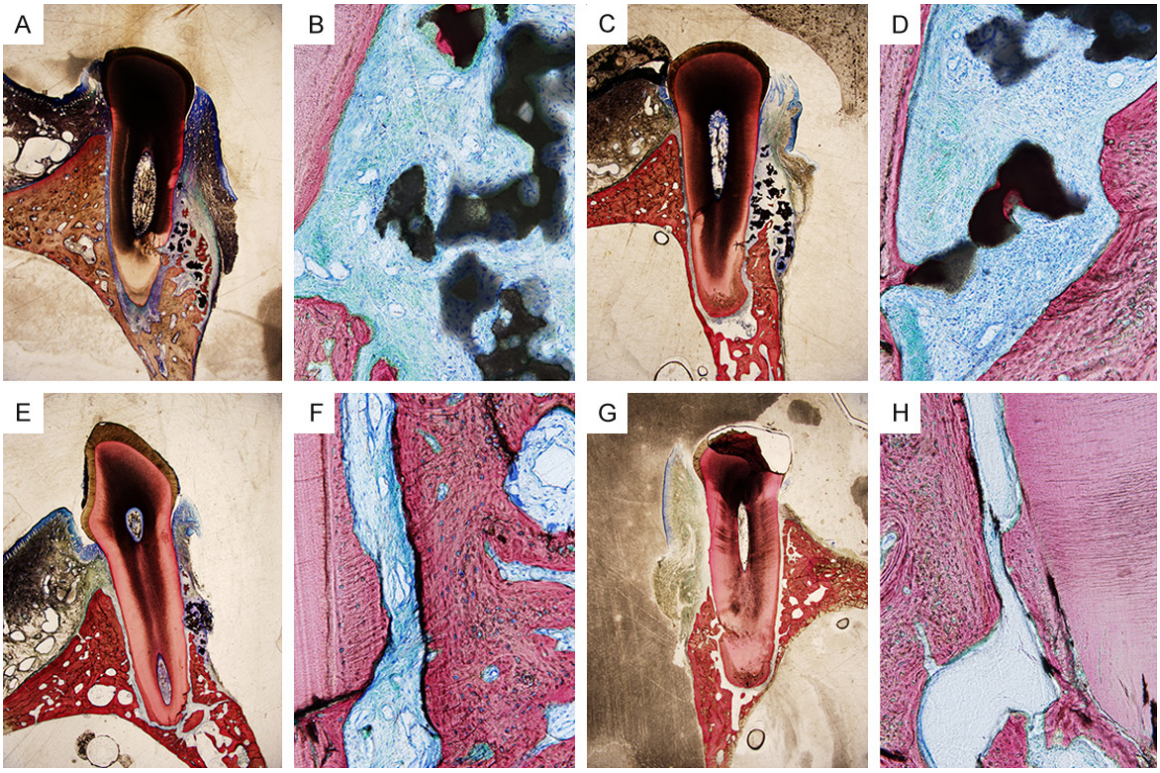


**Figure 6.** Histological analysis of the tissue regeneration in the PDLSCs/BCP group at 12th week (A-F), and that of the OFD group (G, H).

fold with cells and/or loading with proteins (e.g. growth factors or cytokines) in order to improve the regenerative potential of the bone graft. The scaffold acts as a template to preserve tissue volume and shape, as a source of graft cells and is replaced by native tissue over time [17, 18].

In this study, based on the concept of tissue engineering, we focused on the two crucial elements, the PDLSCs and the improved BCP, and their combination and interplay during periodontium reconstruction. Our results showed that the incorporation of PDLSCs and the improved BCP significantly restored the lost

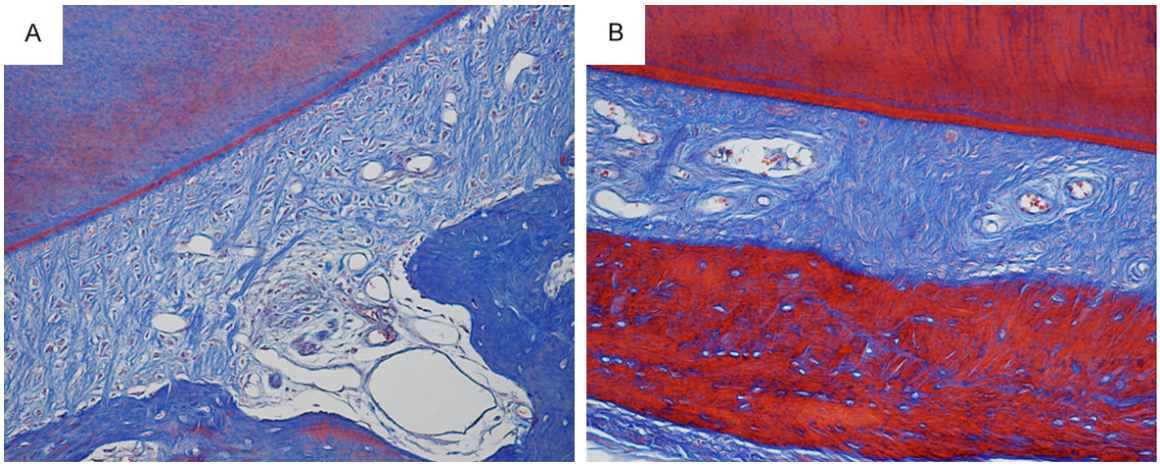


**Figure 7.** Masson staining of alveolar bone of the 8th (A) and 12th (B) week after operation during periodontal regeneration period.

periodontium. The study indicates that the improved BCP is one kind of promising bioactive materials with osteogenesis differentiation of PDLSCs for periodontal tissue regeneration applications.

Since Seo et al. [12] isolated a population of multipotent stem cells in human PDL (PDLSCs), a unique reservoir of stem cells from an accessible tissue resource has been provided. The PDLSCs we collected from root surface exhibited mesenchymal stem cells characteristics. Besides clonogenicity and high proliferation, positive for the early mesenchymal stem cell marker STRO-1 made separation and purification possible using immunomagnetic beads (IMB). Also, as a result of mineralized nodules and greater ALP activity when incubated in osteogenic medium, we confirmed the PDLSCs have the potential of osteogenic differentiation. Recent studies have indicated that the paracrine effects of the growth factors and cytokines secreted from implanted MSCs may promote tissue regeneration *in vivo* [19]. However PDLSCs were not labeled *in vivo*, making it impossible to assess whether the PDLSCs contributed directly to the new periodontal tissues or whether they enhanced the activity of endogenous progenitor cells through the production of bioactive factors. Both of these two hypotheses make the PDLSCs potential cells for periodontal tissue regeneration.

Gazdag et al. defined the following requirements for an optimal graft material: a three dimensional, porous, osteoconductive matrix that allows ingrowth of bone progenitor cells and vascularisation, osteoinductive factors that recruit progenitor cells from the host tissue and induce bone formation, graft cells capable of differentiating into osteoblasts and mechanical strength to ensure tissue integrity until the bone healing process is completed [20, 21].

Synthetic bone substitute materials have to be biocompatible, biodegradable, osteoconductive and processable into macroporous scaffolds tailored to the specific defect [22, 23]. Besides material composition, an important characteristic of scaffolds that shall promote tissue ingrowth and new bone formation is their macrostructure. Cell migration and tissue penetration into the scaffold require a minimum pore size of 50-100 μm; an optimal ingrowth of osteoblast cells requires pore sizes of 200-400 μm [24, 25].

The improved BCP composited by HA and β-TCP at the weight ratio of 40:60 was one kind of nano-powder with constituent dimensions of 30-50 nm. It had abundant micro pores that are distributed widely in the walls of macro pores, with a mean pore diameter of 162 μm and porosity high up to 80%. Sufficient pore size allowed cells to migrate or adhere on the surface layer of a material, whereas interconnecting pores permitted cells to grow into the interior region of the scaffold. Our scaffold conformed to the design features of cell delivery, which involve an internal structure compatible with cell attachment and colonization, as well as permitting the ingrowth of tissues compati-

ble with those to be regenerated [26]. Furthermore, the interconnecting pores formed assess to defect region for nutrient transportation meanwhile promoting angiogenesis. As discussed by previous researchers, the seeding density attaining to eventual osteogenesis should be no less than $5.0 \times 10^5$ cells/ml. The form of the improved BCP was granulated block, thus we measured the density by mass referring to Gronthos's work [27]. Cells were resuspended in the medium without FBS at a density of $5 \times 10^6$ cells/20 mg BCP, and then dropped onto the BCP by means of the pipetting technique. This previous experiment *in vitro* demonstrated that PDLSCs can be well proliferated on the improved BCP, consequently it paved the way for further implantation *in vivo*.

The defect district we set at the buccal aspect aimed to mimic the most frequent periodontium loss in clinic. Micro-CT, as a nondestructive technique, was adopted to assess the visual change of buccal alveolar bone formation over conventional X-ray plain film since it enabled three dimensions reconstruction of two dimensions images which were recorded by cone-beam type X-ray CT. Compared to fan-beam X-ray CT, cone-beam micro-CT is available to measure μ more precisely and accurately in three dimensions; this is due to its extremely high spatial resolution enhanced utilization rate of radiation. Results were analyzed by micro-CT, to contrast whether there was significant difference between two groups. The PDLSCs/BCP group has achieved marked alveolar height regain after 12 weeks compared with control group, although there was a small amount of complex left. We deduced that associated with the length of healing period. It should be improved in further studies.

Fluorescence labeling was applied to visualize newly formed bone tissues. For example, since the 1950s, tetracycline (TC) administration has been used to create fluorescent 'labels' in bone for histomorphometric analysis. *In vivo*, tetracycline labels form due to natural fluorescence and chemical affinities for hard tissues [28].

Single labeling cannot reflect the bone deposit rate while multiple injections make it difficult to distinguish stripes in accordance with time sequence. Harris et al. [29] first introduced two stain agents labeling to make distinctions between coloration stripes. Thanks to calcein green and xylenol orange which have similar property to oxytetracycline, they were present in the healing bone of the transverse process and marked the areas of bone tissue regeneration in sequence. In the PDLSCs/BCP group, the staining region displayed irregular along with degradation of material. Nevertheless, the OFD group presented regular parallel marked lines due to metabolism.

At the 8th week after operation during periodontal regeneration period in experimental group, alveolar bone, the new bone regenerated by using BCP was mainly blue, indicating that the maturity of new alveolar bone did not reach the normal level. At the 12th week after operation during periodontal regeneration period in experimental group, the alveolar bone was red and blue, indicating that the maturity changed during the process of bone remodeling. When the bone tissue grown from new to mature, the collagen got aged, and more regular arrangement, more compact, and more linkage, leading to changes in charge characteristic and staining. Thus, more red indicated higher maturity. In Masson staining of mature bone, the collagen was red, and the new bone was red and blue during maturation. This study could clearly reveal the maturation of new bone and collagen during periodontal regeneration period through Masson staining. Thus, it can be inferred that periodontal regeneration was success.

As to the volume of periodontal regeneration depended on many factors, such as material property, position of defect, study period, and so on. The choice of surgical district will be a direct impact on the effectiveness of regeneration. The reason of district definition in our study is that buccal aspect dehiscence is the most common periodontium loss in our clinical treatment, however, few literatures reported the therapy on it. Though the volume of periodontal regeneration in this study was still far to ideal, the efficacy of the improved BCP is positive.

## Conclusion

The improved BCP works as a scaffold to provide space for periodontal tissue formation, and as a barrier to obstruct epithelium invading. To combine with PDLSCs, it is proved to be efficient for tissue engineering. In addition, it

may be suitable carrier of various growth factors for tissue engineering. For orthodontists, we pay more attention to the function of newly regenerated periodontium and its possibility to be served as substance for orthodontic teeth movement.

## Acknowledgements

This study was supported by grants from the National Natural Science Foundation of China, 30901697 (2009).

## Disclosure of conflict of interest

None.

**Address correspondence to:** Wenyi Zong, Department of Orthodontics, School & Hospital of Stomatology, Tongji University, Shanghai Engineering Research Center of Tooth Restoration and Regeneration, Shanghai 200072, China. E-mail: dot.zong@hotmail.com

## References

[1] Helgeland E, Shanbhag S, Pedersen TO, Mustafa K and Rosen A. Scaffold-based TMJ tissue regeneration in experimental animal models: a systematic review. Tissue Eng Part B Rev 2018; 24: 300-316.

[2] Rabkin E and Schoen FJ. Cardiovascular tissue engineering. Cardiovasc Pathol 2002; 11: 305-317.

[3] Batouli S, Miura M, Brahim J, Tsutsui TW, Fisher LW, Gronthos S, Robey PG and Shi S. Comparison of stem-cell-mediated osteogenesis and dentinogenesis. J Dent Res 2003; 82: 976-981.

[4] Hutmacher DW. Scaffolds in tissue engineering bone and cartilage. Biomaterials 2000; 21: 2529-2543.

[5] Chen Y, Wang J, Zhu XD, Tang ZR, Yang X, Tan YF, Fan YJ and Zhang XD. Enhanced effect of beta-tricalcium phosphate phase on neovascularization of porous calcium phosphate ceramics: in vitro and in vivo evidence. Acta Biomater 2015; 11: 435-448.

[6] Arcos D, Izquierdo-Barba I and Vallet-Regi M. Promising trends of bioceramics in the biomaterials field. J Mater Sci Mater Med 2009; 20: 447-455.

[7] Barrere F, van Blitterswijk CA and de Groot K. Bone regeneration: molecular and cellular interactions with calcium phosphate ceramics. Int J Nanomedicine 2006; 1: 317-332.

[8] Duan YR, Zhang ZR, Wang CY, Chen JY and Zhang XD. Dynamic study of calcium phosphate formation on porous HA/TCP ceramics. J Mater Sci Mater Med 2004; 15: 1205-1211.

[9] Xin R, Leng Y, Chen J and Zhang Q. A comparative study of calcium phosphate formation on bioceramics in vitro and in vivo. Biomaterials 2005; 26: 6477-6486.

[10] Olton D, Li J, Wilson ME, Rogers T, Close J, Huang L, Kumta PN and Sfeir C. Nanostructured calcium phosphates (NanoCaPs) for non-viral gene delivery: influence of the synthesis parameters on transfection efficiency. Biomaterials 2007; 28: 1267-1279.

[11] Shi H, Ma J, Zhao N, Chen Y and Liao Y. Periodontal regeneration in experimentally-induced alveolar bone dehiscence by an improved porous biphasic calcium phosphate ceramic in beagle dogs. J Mater Sci Mater Med 2008; 19: 3515-3524.

[12] Seo BM, Miura M, Gronthos S, Bartold PM, Batouli S, Brahim J, Young M, Robey PG, Wang CY and Shi S. Investigation of multipotent postnatal stem cells from human periodontal ligament. Lancet 2004; 364: 149-155.

[13] Nagatomo K, Komaki M, Sekiya I, Sakaguchi Y, Noguchi K, Oda S, Muneta T and Ishikawa I. Stem cell properties of human periodontal ligament cells. J Periodontal Res 2006; 41: 303-310.

[14] Hernandez-Monjaraz B, Santiago-Osorio E, Monroy-Garcia A, Ledesma-Martinez E and Mendoza-Nunez VM. Mesenchymal stem cells of dental origin for inducing tissue regeneration in periodontitis: a mini-review. Int J Mol Sci 2018; 19.

[15] Gauthier O, Muller R, von Stechow D, Lamy B, Weiss P, Bouler JM, Aguado E and Daculsi G. In vivo bone regeneration with injectable calcium phosphate biomaterial: a three-dimensional micro-computed tomographic, biomechanical and SEM study. Biomaterials 2005; 26: 5444-5453.

[16] Hildebrand T, Laib A, Muller R, Dequeker J and Ruegsegger P. Direct three-dimensional morphometric analysis of human cancellous bone: microstructural data from spine, femur, iliac crest, and calcaneus. J Bone Miner Res 1999; 14: 1167-1174.

[17] Itthichaisri C, Wiedmann-Al-Ahmad M, Huebner U, Al-Ahmad A, Schoen R, Schmelzeisen R and Gellrich NC. Comparative in vitro study of the proliferation and growth of human osteoblast-like cells on various biomaterials. J Biomed Mater Res A 2007; 82: 777-787.

[18] Qasim SB, Delaine-Smith RM, Fey T, Rawlinson A and Rehman IU. Freeze gelated porous membranes for periodontal tissue regeneration. Acta Biomater 2015; 23: 317-328.

[19] Inukai T, Katagiri W, Yoshimi R, Osugi M, Kawai T, Hibi H and Ueda M. Novel application of

stem cell-derived factors for periodontal regeneration. Biochem Biophys Res Commun 2013; 430: 763-768.
[20] Gazdag AR, Lane JM, Glaser D and Forster RA. Alternatives to autogenous bone graft: efficacy and indications. J Am Acad Orthop Surg 1995; 3: 1-8.
[21] Zipfel GJ, Guiot BH and Fessler RG. Bone grafting. Neurosurg Focus 2003; 14: e8.
[22] Bartold PM, Xiao Y, Lyngstaadas SP, Paine ML and Snead ML. Principles and applications of cell delivery systems for periodontal regeneration. Periodontol 2000 2006; 41: 123-135.
[23] Marcacci M, Kon E, Moukhachev V, Lavroukov A, Kutepov S, Quarto R, Mastrogiacomo M and Cancedda R. Stem cells associated with macroporous bioceramics for long bone repair: 6- to 7-year outcome of a pilot clinical study. Tissue Eng 2007; 13: 947-955.
[24] Fan W, Crawford R and Xiao Y. Enhancing in vivo vascularized bone formation by cobalt chloride-treated bone marrow stromal cells in a tissue engineered periosteum model. Biomaterials 2010; 31: 3580-3589.
[25] Boyan BD, Hummert TW, Dean DD and Schwartz Z. Role of material surfaces in regulating bone and cartilage cell response. Biomaterials 1996; 17: 137-146.
[26] Chen FM, Sun HH, Lu H and Yu Q. Stem cell-delivery therapeutics for periodontal tissue regeneration. Biomaterials 2012; 33: 6320-6344.
[27] Gronthos S, Mankani M, Brahim J, Robey PG and Shi S. Postnatal human dental pulp stem cells (DPSCs) in vitro and in vivo. Proc Natl Acad Sci U S A 2000; 97: 13625-13630.
[28] Fernandez-Flores A, Nguyen T and Cassarino DS. Mucocutaneous hyperpigmentation in a patient with a history of both minocycline and silver ingestion. Am J Dermatopathol 2017; 39: 916-919.
[29] Harris WH, Travis DF, Friberg U and Radin E. The in vivo inhibition of bone formation by Alizarin Red S. J Bone Joint Surg Am 1964; 46: 493-508.